ELSEVIER

Colloids and Surfaces
A: Physicochemical and Engineering Aspects 156 (1999) 49–64

COLLOIDS AND SURFACES A

www.elsevier.nl/locate/colsurfa

Investigation of the oscillating bubble technique for the determination of interfacial dilatational properties

Thodoris D. Karapantsios [a,*], Margaritis Kostoglou [b]

[a] *Department of Mechanical and Industrial Engineering, University of Thessaly, Pedion Areos, GR-38334 Volos, Greece*
[b] *Chemical Process Engineering Research Institute, P.O. Box 1517, 540 06 University City, Thessaloniki, Greece*

Received 5 May 1998; received in revised form 24 July 1998; accepted 30 July 1998

Abstract

A mathematical framework is developed for measuring the dilatational rheological properties of gas-liquid interfaces by analyzing small amplitude radial oscillations of an air bubble blown into a liquid substrate. Contrary to earlier analyses which customarily require the bubble radius change during the oscillation, the present study is based on the readily measurable quantities of bubble pressure change during the oscillation and phase lag between the bubble pressure and the relative displacement of the oscillation generating device. To expose the extensive interrelationships among the various experimental parameters that have a profound effect on bubble dynamics, the analysis is focused on the influence of the variable gas volumes at the sides of the differential pressure transducer, the gas phase compressibility, the dynamic behavior of the transducer membrane and the bubble surface being only a segment of a sphere, as they play a key role in the response of the system. A linear viscoelastic surface behavior is assumed which includes intrinsic surface viscosities and Gibbs elasticities. New data are deduced from previous measurements on the dilatational surface properties of stearic acid monolayers which, being practically insoluble in water, offer an ideal experimental system without the complications due to bulk-interface interactions. For a fixed frequency of oscillation, a virtually constant dilatational surface viscosity is determined throughout the employed concentration range. Yet, surface viscosity is found to slightly increase when the oscillation frequency increases. In addition, for the range of the examined parameters, no firm evidence of a dilatational surface elasticity is observed.

Keywords: Oscillating bubble method; Interfacial dilatational properties; Bubble surfactants; Surface rheology; Stearic acid

1. Introduction

When an interface containing surfactant is at rest, the interfacial stress is composed only of the interfacial tension which assumes its equilibrium value. Under dynamic conditions though, the interfacial stress is determined by both interfacial tension and dynamic rheological properties. These dynamic properties are generally classified as either compositional or intrinsic [1–3]. During dynamic processes the interface may be stretched or compressed locally or convective motion may re-

* Corresponding author.

0927-7757/99/$ - see front matter
PII: S0927-7757(99)00013-8

distribute material in the interface. The net effect is the development of interfacial concentration gradients which cause local variations in the interfacial tension over the interface. These lateral variations in interfacial tension may act to enhance or retard the motion of the system. In either case, the effects appear to be due to dynamic interfacial properties such as elasticity and viscosity. However, because their origin is due to redistribution of surfactant and the strong relationship between surface tension and surface concentration, these properties are termed compositional.

In addition to the effects of induced variations in interfacial tension sustained by mass transfer limitations, resistance to interfacial deformation may occur due to the existence of intrinsic hydrodynamic properties of the interface, attributable most likely to intermolecular interactions between surfactant molecules. The coupling of compositional and intrinsic effects adds complexity to any experimental investigation which desires to study them independently, and distinguish between them in an unambiguous way.

The resistance of an interface to an isotropic area deformation is proportional to dilatational interfacial properties. These properties appear to be particularly important in many situations in practice where interfaces are being stretched, such as in continuous film coating processes, film drainage in coalescence and foam stability processes, oil displacement from sandstone pores by chemical flooding and pulmonary dynamics [4].

In an attempt to measure the interfacial dilatational properties, the radially oscillating bubble technique has been introduced [5–7]. The technique calls for the generation of an air bubble on the tip of a capillary tube immersed in an external phase. The bubble is subjected to periodic volumetric oscillations and the resulting periodic change of the pressure across the interface and the phase lag between the bubble pressure and the bubble radius have been customarily proposed as the parameters from which the interfacial properties can be determined.

From the viewpoint of measuring dilatational surface properties, it is obvious that this experimental technique offers a number of advantages over others. For small bubbles, interfacial stress will dominate gravitational effects, resulting in a bubble that is almost spherical. Thus, any increase or decrease in bubble size will result in a nearly isotropic expansion or compression of the interface, thereby isolating dilatational properties from shear properties. Also, the analysis of the experimental data is straightforward, because the spherical geometry greatly simplifies the equations for the bulk phases and the interface.

The first to report the use of this method for dilatational studies of dynamic interfacial behavior were Kretzschmar and Lunkenheimer [8,9]. The theoretical analysis describing the previous experiments was presented by Wantke et al. [10,11]. These pioneering studies were followed by other publications which introduced either new design of apparatuses to monitor the pressure changes inside the bubble or improved the theoretical treatment of the derivation of interfacial properties [12–20]. However, the experiment was always limited to cases of soluble surfactant solutions, while appreciable measuring errors, speculated to be due to alterations of the contact line of the bubble at the capillary tip [18,20], shed doubt on the accuracy of the results. Furthermore, for all systems examined the bubble surface was assumed to exhibit solely compositional properties.

A more systematic theoretical approach on the bubble technique, which included both compositional and intrinsic properties, was presented by Gottier et al. [21]. They considered the surface layer to obey a linear viscoelastic law. Small amplitude oscillations were employed in order to simplify the algebra. The equations were, then, solved analytically under various adsorption-diffusion kinetics utilizing the bubble pressure amplitude and the phase shift between the bubble radius and the bubble pressure to obtain quantitative information. The recent theoretical work by Johnson and Stebe [22] somehow complemented the previous study by developing a handy mathematical protocol for determining the interfacial properties from the response of an experimental system. Yet, their experiments [17] were limited to a soluble surfactant with no evidence of intrinsic surface properties. Nevertheless, Johnson and Stebe [17] were among the first to experimentally

demonstrate that the phase angle between bubble radius and gas pressure is amenable to precise quantitative interpretation for measuring dynamic interfacial properties. In the above studies, the bubble was always considered as a closed shaped perfect sphere which performs purely radial oscillations about an equilibrium state. The fact that a bubble in a real experiment, being attached at the tip of a capillary tube, is only a segment of a sphere which, in principle, does not expand and contract in a purely radial fashion due to contact line limitations, was never discussed.

To our knowledge, the only version of the oscillating bubble technique that involves insoluble surfactants is the one presented by Palmer and co-workers [23–25]. A considerable experimental advantage in these studies lies in the ease with which account could be taken of the surface tension contribution to the bubble pressure change during the oscillation by a compensatory pressure signal on the reference side of the measuring differential pressure transducer. The benefit of this technique is not simply that the surface dilatational properties can now be measured directly, but that a more sensitive range of the transducer can be used as well. In addition, a new idea was tested: the amplitude of bubble pulsation was estimated from the position of the oscillation generating device (a syringe), an approach which allowed to register any shift of the bubble contact line at the tip of the capillary tube just by comparing the syringe volume variation with the resulting pressure change. In these studies, the theoretical analysis was simplified by assuming a purely viscous surface behavior and intrinsic dilatational viscosity values were inferred exclusively from measurements of pressure drop across the bubble interface during the oscillation. Moreover, only dilute monolayers ($>120\text{Å}^2$/molecule) were achieved, because of experimental constraints.

Ko [23], working at a fixed oscillation frequency of 6 cycles/min, determined an unexpectedly high dilatational viscosity of about 40 mNs/m for palmitic acid. Karapantsios [24] working with stearic acid monolayers, improved upon the technique of Ko by refining certain experimental deficiencies and expanded the frequency range to 100 cycles/min. An important new feature of the latter study was the simultaneous measurement of the bubble pressure and the phase lag between the amplitude of the bubble pressure and the position of the oscillation generating syringe. However, just the bubble pressure signal was used for data reduction purposes; the measured phase lag only served as an independent check of accuracy for the values of the interfacial properties. The values of the dilatational viscosity obtained for stearic acid monolayers were between 3 and 20 mNs/m, decreasing with both surface coverage and oscillation frequency.

Our critical review of the work by Palmer and his co-workers [23–25] suggests that although their experiment had the potential to isolate and measure accurately the surface dilatational properties, the employed data reduction procedure was rather inadequate to produce reliable results. This is manifested in several ways: (a) the estimated values of the dilatational viscosity for all tested substances were much higher than other reported results; (b) the comparison between measured and predicted phase lags between bubble pressure and syringe movement in Karapantsios's work [24], showed a remarkable discrepancy; and (c) Karapantsios's experiments conducted with bubbles blown in surfactant-free substrates, produced non-zero viscosity values for clean interfaces. These anomalies may be explained, at least in part, if the bubble pressure signal, which was the basic experimental parameter in their model equations, is not a satisfactory indicator of surface rheology, just by itself. Anyhow, it is felt that additional effort is required to describe the dynamic behavior of the oscillating bubble.

The present work is primarily concerned with improving the work of Palmer and co-workers by offering an improved mathematical framework for the determination of interfacial dilatational properties which is based not only on the amplitude of the bubble pressure but also on the phase lag between the bubble pressure and the position of the oscillation generating syringe. Note that phase lag measurements have not been adequately explored in the literature so far. Furthermore, in order to deduce the values of interfacial properties, an analytical theoretical model is developed

incorporating both intrinsic viscosities and compositional (Gibbs) elasticities. Emphasis is given to studying the influence of the contiguous gas phase compressibility, the variable gas volumes at the sides of the differential pressure transducer, the dynamic behavior of the transducer membrane and the bubble surface being only a segment of a sphere. Ultimately, new values of interfacial properties of stearic acid monolayers are presented by recalculating data obtained by Karapantsios [24].

2. General apparatus characteristics

In Fig. 1 the experimental configuration by Karapantsios [24] is presented schematically. A small air bubble is formed at the tip of a capillary tube, which protrudes vertically into a glass chamber (test cell) containing the surrounding liquid phase. The capillary tube is connected to the measuring side of a differential pressure transducer. A syringe is also incorporated into the plumbing that is attached to each side of the pressure transducer. The plungers of the syringes can be made to move independently but synchronously, according to selectable oscillation modes. The pulsation of the measurement-side syringe plunger creates the periodic deformation of the bubble caused by the influx and efflux of air through the capillary tube. The resulting periodic change of the internal bubble pressure is monitored by the differential pressure transducer. The reference-side syringe plunger is also able to pulsate periodically in a fashion synchronous with the measuring-side one, simulating a pressure signal on the reference side of the transducer which resembles the pressure change inside a bubble that occurs due solely to the surface tension variation. Simulation of the surface tension effect on the reference side, would allow the differential pressure transducer to detect the signal due to the surface and bulk viscosities only.

It must be noted that the amplitude of the bubble oscillations in Karapantsios's experiment is not registered by an optical means but a procedure is developed to evaluate it from the very precise knowledge of the computer controlled motion of the oscillation generating syringe. This technique, successfully contrasted to traditional optical registration through a telescope lenses for very low frequencies of oscillation [24], seems to offer a tempting alternative for the prompt registration of bubble radius with apparent advantages over the cumbersome image analysis as regards convenience and labor. The residual uncertainty due to the indirect way of evaluating the bubble radius is always less important than issues associated with the non-sphericity of the bubble, the translation of the center of the bubble and the movement of the contact line [24]. Nevertheless, the present analysis should be tested further over a broader range of experimental parameters before conclusive statements can be made. Besides, by viewing the bubble through the telescope lenses, Karapantsios developed a record of bubble radius versus time during the oscillation. This information was used primarily to determine the equilibrium bubble radius, assure stable operational conditions and bubble sphericity, and occasionally for comparisons with the algorithm which supervises the computer driven displacement function of the syringes [24].

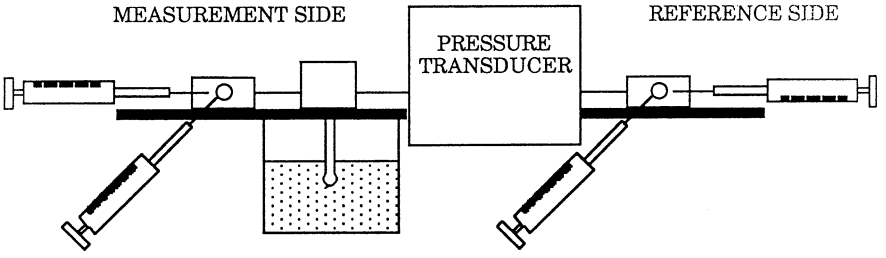

Fig. 1. Schematic diagram of the experimental apparatus of Karapantsios [24].

Perhaps the major concern in such experiments is the construction of the capillary tip to which the bubble is attached and which is deemed responsible for the stability of the three phase contact line [20]. The free end of Karapantsios's capillary tube is machined to be a knife-edged circle, slightly tapered at the inside; several tests are tried to make it non-wettable. Surface concentration is estimated from the portion of the monolayer captured by the end of the capillary tube as it is brought to touch the water substrate and from the surface area of the bubble which is blown thereafter. Description of the experiment is given elsewhere [24].

3. Theory

3.1. Constitutive equation

Consider a spherically symmetric bubble, surrounded by an external liquid phase, on which a periodic volume oscillation is imparted. In such a case, the flow around the bubble is purely radial and the interface is uniformly deformed retaining its shape. Excluding all interfacial rheology effects, the equation that describes the pressure difference between the air in the bubble, P_X, and the liquid far from the interface, P_L, is given by the well known Rayleigh-Plesset equation:

$$P_X - P_L = \frac{2\sigma}{R} + 4\mu_w \frac{R'}{R} + \rho_w\left(RR'' + \frac{3}{2}R'^2\right) \quad (1)$$

where R is the instantaneous radius, σ is the interfacial tension, μ_w is the liquid bulk viscosity, ρ_w is the liquid density and prime ($'$) denotes differentiation with respect to time. The last two terms on the RHS of Eq. (1) represent the inertia effects created by the motion of the bubble. Inclusion of these terms in the analysis is, in principal, necessary since only then is P_L the actually measurable pressure on the liquid side far away from the interface. Thus, former analyses [21,22] not including these terms are not generally applicable in every real experiment. Some further comments are presented with respect to Eqs. (24a) and (24b).

If, in addition to any surface tension related compositional contribution, the interface is further assumed to exhibit a Newtonian intrinsic behavior, then Scriven's [26] model can be used to describe the normal stresses at the interface and Eq. (1) becomes:

$$P_X - P_L = \frac{2\sigma}{R} + 4\left(\frac{\kappa}{R} + \mu_w\right)\frac{R'}{R} + \rho_w\left(RR'' + \frac{3}{2}R'^2\right) \quad (2)$$

where κ is the intrinsic dilatational viscosity of the interface. For those experimental configurations [23,24], where the hydrostatic pressure in the region of the bubble is negligible, it can be further assumed that $P_L \cong 1$ atm.

3.2. Mathematical formulation of the experimental technique

With the transducer connected to the apparatus, the enclosed air volumes include not only the dead spaces in the transducer but also the air in the tubing and connections. Therefore, due to air compressibility, the volume displaced by the syringe does not equal the change in bubble volume. Furthermore, the pressure on both sides of the transducer is affected not only by the movement of the syringes but also by the extent to which the corresponding air-volume is changed by the deflection of the transducer membrane. To account for these and other, more subtle, effects an analysis is done, based on the following assumptions: (a) the bubble is essentially spherical, (b) the translation of the bubble center during the oscillation is negligible and (c) no surfactant exchange between the interface and the adjacent phases takes place.

The instantaneous total volume of the measurement side V_X,

$$V_X = V_X^a + V^b + V_X^s + V^m \quad (3)$$

where V_X^a and V_X^s are the dead air volume and the volume of the syringe in the measuring side, V^b is the volume of the bubble and V^m is the volume created by the diaphragm deflection. Accordingly, for the reference side the total volume V_R is

$$V_R = V_R^a + V_R^s - V^m \quad (4)$$

Contrary to the few theoretical studies dealing with oscillating bubbles [21,22] where the bubble was treated as a closed surface, here it is well recognized that a bubble blown out of a tube is actually a segment of a sphere. This strongly implies two things: due to the inevitable translation of the center of the bubble during the oscillation, the motion of the bubble is not purely radial and therefore the redistribution of material across the interface is not uniform; possible movement of the contact line during the oscillation alters the correspondence between bubble radius and pressure due to change of surface concentration. As a result, for such bubbles it has been suggested that the bulk contribution (viscous and inertia terms) in Eq. (1) must be determined by appropriate calibration measurements [10–12]. This indeed is more accurate for the case of incomplete spheres but introduces appreciable perplexity in the quantitative analysis of the measurements. Besides, there is some experimental evidence [22–24] that for bubbles larger than a hemisphere, as those encountered in this study, the translation of the bubble center is much less than with bubbles smaller than a hemisphere [10–12].

Simple analytic geometry leads to the following expressions for the volume and the surface area of the bubble:

$$V^b = \frac{\pi}{3}(2R^3 + (2R^2 + R_c^2)(R^2 - R_c^2)^{1/2}) \quad (5a)$$

$$A^b = 2\pi(R^2 + R(R^2 - R_c^2)^{0.5}) \quad (5b)$$

where R_c is the capillary tube radius.

The diaphragm deflection of the pressure transducer results in a dynamic volume effect which for small pressure changes can be represented by a linear relationship of the form:

$$V^m = K_m(P_X - P_R) \quad (6)$$

where K_m is a constant and P_X and P_R are the instantaneous pressures on the measurement and reference side of the transducer, respectively. Karapantsios [24] evaluated the membrane constant and the dead air-volumes on both sides of the transducer through calibration experiments as follows: $K_m = 0.19$ μl/Pa, $V_X^a = 1735$ μl and $V_R^a = 4650$ μl.

The externally controlled periodic change of the volume of the two syringes is

$$V_X^s = D\sin(\omega t) \quad (7a)$$

$$V_R^s = \lambda D\sin(\omega t) \quad (7b)$$

where D is one half the amplitude of the applied function, λ is a positive number, ω is the oscillation frequency and t is the instantaneous time.

The behavior of the air during the compression-expansion process may vary between two extreme cases, namely the isothermal and the adiabatic behavior. The general gas compressibility equations that describe the air behavior are

$$P_X(V_X)^\beta = K_X^g \quad (8a)$$

$$P_R(V_R)^\beta = K_R^g \quad (8b)$$

where K_X^g and K_R^g are constants, $\beta = 1$ for isothermal behavior and $\beta = 1.403$ for adiabatic behavior. Air is taken to behave adiabatically for all experimental conditions although trials with air assumed to behave isothermally did not give much different results which are definitely within the range of accuracy of the measurements. This observation supports the assumption of an ideal gas behavior for the enclosed air volumes which is not surprising for such low pressures. Besides, the size of the gas chamber on both sides of the transducer is small regarding the respective acoustic wave. Some further experimental support is provided in Section 4.1.

Substituting Eqs. (3), (4), (5a), (5b), (6), (7a) and (7b) in Eqs. (8a) and (8b) the following relations are taken

$$P_X(V_X^a + V^b + D\sin(\omega t) + K_m(P_X - P_R))^\beta = K_X^g \quad (9a)$$

$$P_R(V_R^a + \lambda D\sin(\omega t) - K_m(P_X - P_R))^\beta = K_R^g \quad (9b)$$

Prior to pulsation, when both the syringes are still and the bubble remains immobile, the system is considered in static equilibrium. This equilibrium is assumed as the reference state initial conditions ($t = 0$). In this case, the Young-Laplace equation gives (the subscript '0' indicates initial equilibrium)

$$P_{X_0} - P_L = \frac{2\sigma}{R} \tag{10}$$

The following relations are also valid for equilibrium conditions

$$V_{X_0} = V_X^a + V_0^b + V_0^m \tag{11a}$$

$$V_{R_0} = V_R^a - V_0^m \tag{11b}$$

$$V_0^m = K_m(P_{X_0} - P_{R_0}) \tag{11c}$$

$$P_{X_0}(V_{X_0})^\beta = K_X^g \tag{11d}$$

$$P_{R_0}(V_{R_0})^\beta = K_R^g \tag{11e}$$

The main variables are decomposed to equilibrium and perturbation parts as follows:

$$P_X = P_{X_0} + P_{X_1} \tag{12a}$$

$$P_R = P_{R_0} + P_{R_1} \tag{12b}$$

$$R = R_0 + R_1 \tag{12c}$$

$$V^b = V_0^b + uR_1 \tag{12d}$$

where

$$u = \left(\frac{dV^b}{dR}\right)_{R_0} = \frac{\pi}{3}\,[6R_0^2 + 4R_0(R_0^2 - R_c^2)^{0.5} + 4R_0(2R_0^2 + R_c^2)(R_0^2 - R_c^2)^{0.5}] \tag{13}$$

Eqs. (9a) and (9b) are divided by V_{X_0} and V_{R_0}, respectively, and after substitution of the perturbation variables they are modified as

$$(P_{X_0} + P_{X_1}) \times \left[1 + \frac{uR_1 + D\sin(\omega t)}{V_{X_0}} + \frac{K_m}{V_{X_0}}\,(P_{X_1} - P_{R_1})\right]^\beta = P_{X_0} \tag{14a}$$

$$(P_{R_0} + P_{R_1}) \times \left[1 + \frac{\lambda D\sin(\omega t)}{V_{R_0}} - \frac{K_m}{V_{R_0}}\,(P_{X_1} - P_{R_1})\right]^\beta = P_{R_0} \tag{14b}$$

The above non-linear system of equations must be solved for the perturbation variables P_{X_1} and P_{R_1}. For small perturbations it can be linearized. The linearized result is:

$$P_{X_1} = k_1\left(\frac{u}{V_{X_0}}\,R_1 + \frac{D}{V_{X_0}}\right) + k_2\,\frac{\lambda D}{V_{R_0}}\,\sin(\omega t) \tag{15a}$$

$$P_{R_1} = k_3\left(\frac{u}{V_{X_0}}\,R_1 + \frac{D}{V_{X_0}}\right) + k_4\,\frac{\lambda D}{V_{R_0}}\,\sin(\omega t) \tag{15b}$$

where

$$k_1 = \frac{-\beta P_{X_0}(1 + \beta K_m P_{R_0}/V_{R_0})}{1 + \beta K_m P_{R_0}/V_{R_0} + \beta K_m P_{X_0}/V_{X_0}} \tag{16a}$$

$$k_2 = \frac{-K_m\beta^2 P_{X_0}P_{R_0}/V_{X_0}}{1 + \beta K_m P_{R_0}/V_{R_0} + \beta K_m P_{X_0}/V_{X_0}} \tag{16b}$$

$$k_3 = \frac{-K_m\beta^2 P_{X_0}P_{R_0}/V_{R^0}}{1 + \beta K_m P_{R_0}/V_{R_0} + \beta K_m P_{X_0}/V_{X_0}} \tag{16c}$$

$$k_4 = \frac{-\beta P_{R_0}(1 + \beta K_m P_{X_0}/V_{X_0})}{1 + \beta K_m P_{R_0}/V_{R_0} + \beta K_m P_{X_0}/V_{X_0}} \tag{16d}$$

Taking into account that $R_1 \ll R_o$ and that the oscillation frequency is such that allows the linearization of inertia terms, the expansion of Eq. (2) around the equilibrium state gives:

$$\rho_w R_0 R_1'' + \frac{4}{R_0}\left(\frac{\kappa}{R_0} + \mu_w\right)R_1' + \left(\frac{2\sigma_0}{R_0^2} - \frac{2\Gamma_0 A_p}{R_0 A_0}\right)R_1 = k_1\,\frac{u}{V_{X_0}}\,R_1 + \frac{D}{V_{X_0}}\,(k_1 + k_2\lambda)\,\sin(\omega t) \tag{17}$$

where the following expansion of the surface tension has been used

$$\sigma = \sigma_0 + \left(\frac{d\sigma}{d\Gamma}\right)_0 \Gamma_1 \tag{18}$$

$$\Gamma_1 = \Gamma_0(A_0/A - 1) = -\Gamma_0\,\frac{A_p}{A_0}\,R_1 \tag{19}$$

$$A_p = \left(\frac{dA}{dR}\right)_{R_0} = 2\pi(2R_0 + R_0^2(R_0^2 - R_c^2)^{0.5} + R_0^2(R_0^2 - R_c^2)^{-0.5}) \tag{20}$$

Combining all the above, it is found that the dynamic response of the bubble in our experiment is given by the following second-order linear differential equation:

$$A^*R_1'' + B^*R_1' + C^*R_1 = D^*\sin(\omega t) \quad (21)$$

where

$$A^* = \rho_w R_0 \quad (22a)$$

$$B^* = \frac{4}{R_0}\left(\frac{\kappa}{R_0} + \mu_w\right) \quad (22b)$$

$$C^* = \frac{2\sigma_0}{R_0^2} - \frac{2\Gamma_0 A_p}{R_0 A_0}\left(\frac{d\sigma}{d\Gamma}\right)_0 - k_1\frac{u}{V_{X_0}} \quad (22c)$$

$$D^* = \frac{D}{V_{X_0}}(k_1 + k_2\lambda) \quad (22d)$$

The term $\Gamma_0(d\sigma/d\Gamma)_0$ in Eq. (22c) is the Gibbs dilatational elasticity modulus representing a compositional elastic contribution in the response of the system. This formalism is restricted to insoluble monolayers or measurements at a higher frequency range. If an intrinsic dilatational elasticity, κ'', is also to be accounted for, this would appear as an extra $4\kappa''/R_0^2$ term in the RHS of Eq. (22c). However, the experiments by Karapantsios [24] can not discern between the two elastic contributions and, therefore, only the compositional effect is included in Eq. (22c).

The solution of Eq. (21) is

$$R_1 = K\sin(\omega t) + L\cos(\omega t) \quad (23)$$

where

$$K = D^*\left(C^* - A^*\omega^2 + \frac{\omega^2 B^*}{C^* - A^*\omega^2}\right)^{-1} \quad (24a)$$

$$L = \frac{-\omega B^*}{C^* - A^*\omega^2}K \quad (24b)$$

In many cases the non-linear terms in Eq. (1) are ignored completely. Then the final result in Eqs. (24a) and (24b) does not include the term $A^*\omega^2$. Evidently, this is not a significant point because for realistic frequencies this term is quite small and can be safely ignored. On the other hand, for extremely large frequencies the linear analysis is no longer valid. However the inclusion of the term $A^*\omega^2$ is fundamentally correct because there is always a region of frequencies for which this term is significant whereas the problem retains its linear character.

Finally using Eq. (23), the perturbation pressure difference $\Delta P_m = \Delta P - \Delta P_0$, can be found as

$$\begin{aligned}\Delta P_m &= P_{X_1} - P_{R_1} \\ &= \left(\frac{k_1 u}{V_{X_0}} - \frac{k_3 u}{V_{R_0}}\right)R_1 \\ &\quad + D\left(\frac{k_1 + k_2\lambda}{V_{X_0}} - \frac{k_3 + k_4\lambda}{V_{R_0}}\right)\sin(\omega t) \\ &= E\sin(\omega t) + Z\cos(\omega t)\end{aligned} \quad (25)$$

where

$$E = K\left(\frac{k_1 u}{V_{X_0}} - \frac{k_3 u}{V_{R_0}}\right) + D\left(\frac{k_1 + k_2\lambda}{V_{X_0}} - \frac{k_3 + k_4\lambda}{V_{R_0}}\right) \quad (26a)$$

$$Z = L\left(\frac{k_1 u}{V_{X_0}} - \frac{k_3 u}{V_{R_0}}\right) \quad (26b)$$

From Eq. (25), the difference between the maximum and the minimum bubble pressure during the pulsation and the phase lag between the measured pressure signal and the movement of the syringe are evaluated as

$$\Delta P_{max} = 2E\sin(\varphi) + 2Z\cos(\varphi) \quad (27)$$

$$\varphi = \arctan\left(\frac{E}{Z}\right) \quad (28)$$

To determine the surface dilatational properties in a real experiment a standard procedure is followed. The bubble is forced to pulsate and the change in the pressure differential during the oscillation is recorded continuously. The quantities φ and ΔP_{max} together with the equilibrium bubble radius, the frequency and amplitude of oscillation, are used then as inputs to solve the model-equations. Extensive trial simulations showed that for the range of the employed experimental parameters, ΔP_{max} dictates mainly the values of surface elasticity whereas φ dictates the values of surface viscosity.

3.3. Parametric analysis

To provide insight into the effects of the various physical properties and experimental parameters that are most suspected to be important on bubble dynamics, the descriptive equations are solved next, subject to conditions which are similar to those employed by Karapantsios [24]. The

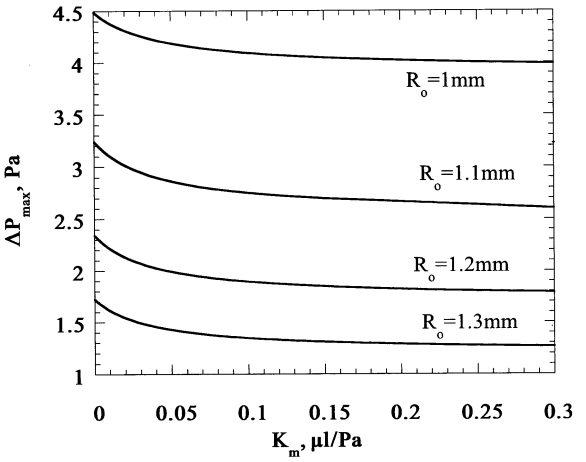

Fig. 2. Effect of pressure transducer's membrane constant on the measured pressure signal ($\sigma_0 = 72$ mN/m; AM = 250 steps; $R_c = 0.83$ mm).

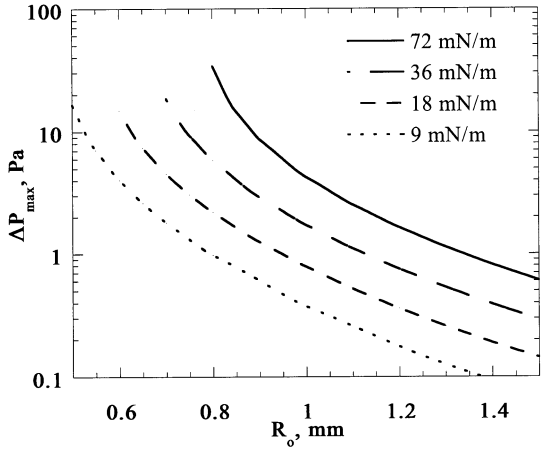

Fig. 3. Surface tension effect on the measured pressure signal with pure interfaces(AM = 250 steps; $R_c = 0.8^* R_0$).

half amplitude of oscillation is $D = 0.5275$ μl (AM = 250 steps) resulting in a change in bubble radius of less than 5–8%, depending on which initial radius is used. Unless otherwise stated, the surface tension and bulk viscosity of the substrate, the oscillation frequency and the capillary tube radius are: $\sigma_0 = 72$ mN/m, $\mu_w = 0.001$ Ns/m^2, $\omega = 20$ cycles/min and $R_c = 0.83$ mm, respectively.

Fig. 2 demonstrates how the experimentally measured pressure signal is affected by the value of the transducer's membrane constant, K_m, at various bubble radii. The value of radii considered, coincide with the values employed experimentally in [24]. It is clear that for values of K_m above 0.15 μl/Pa, small errors in the determination of K_m have only a minor effect and so the bubble pressure change is measured more accurately. This is true for all employed bubble sizes despite their different pressure level. Recall that in [24], K_m was found equal to 0.19 μl/Pa. Two limiting cases are identified in Eqs. (16a), (16b), (16c) and (16d); if $K_m \approx 0$ then:

$$k_1 = -\beta P_{X_0} \tag{29a}$$

$$k_2 = k_3 = 0 \tag{29b}$$

$$k_4 = -\beta P_{R_0} \tag{29c}$$

and if $K_m \approx \infty$ then:

$$k_1 = k_3 = -\beta P_{X_0}\left(1 + \frac{P_{X_0} V_{R_0}}{P_{R_0} V_{X_0}}\right)^{-1} \tag{30a}$$

$$k_2 = k_4 = -\beta P_{R_0}\left(1 + \frac{P_{R_0} V_{X_0}}{P_{X_0} V_{R_0}}\right)^{-1} \tag{30b}$$

If the bubble surface has no rheology, the dynamic response of the bubble is dominated by the surface tension effect, as described by the Young and Laplace equation. This surface tension effect is illustrated in Fig. 3 with respect to equilibrium bubble radius, the lower radius limits being solely due to the perturbation technique, one can proceed further by numerical calculations. Notice that the pressure difference across the transducer membrane is substantial relative to the most sensitive sensor full range of Karapantsios's transducer ([24]; 1.33 Pa; sensitivity 0.001 Pa) even for a surface tension of 9 mN/m. Therefore, it is important to compensate for this pressure on the reference side of the transducer if the objective is to measure very small pressure changes due to the presence of interfacial properties. Assuming that the interface has no dynamic rheological properties and given the oscillation frequencies are less than 100 cycles per second, the maximum pressure difference during the pulsation, ΔP_{max}, is calculated as:

$$\Delta P_{\max} = M\left(\frac{k_1 u}{V_{X_0}} - \frac{k_3 u}{V_{R_0}} \right) + D\left(\frac{k_1 + k_2\lambda}{V_{X_0}} - \frac{k_3 + k_4\lambda}{V_{R_0}} \right) \quad (31a)$$

where

$$M = -\frac{D}{V_{X_0}} (k_1 + k_2\lambda)\left(\frac{2\sigma_0}{R_0^2} + \frac{k_1 u}{V_{X_0}} \right)^{-1} \quad (31b)$$

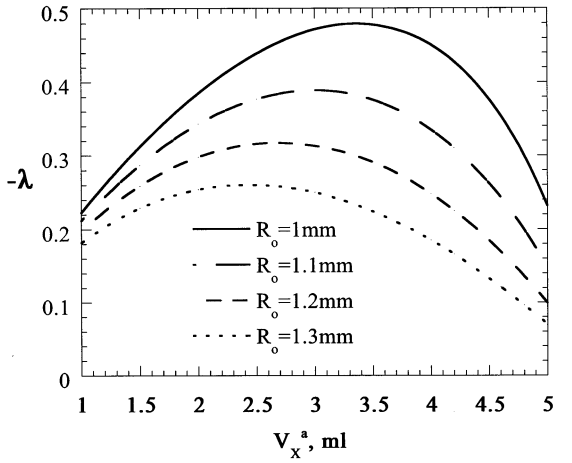

Fig. 4. Reference syringe amplitude for fully compensating the surface tension effect under quasi-static conditions ($\sigma_0 = 72$ mN/m; AM = 250 steps; $R_c = 0.83$ mm).

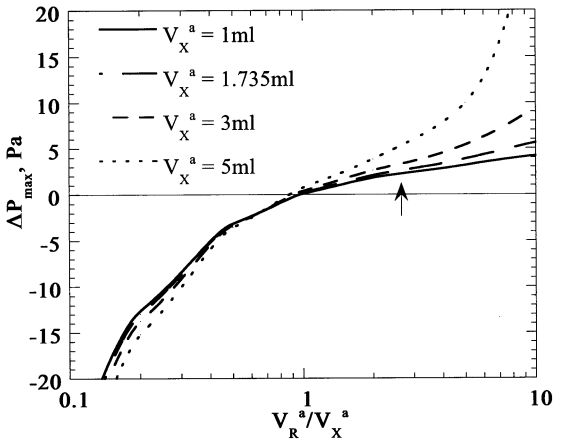

Fig. 5. Effect of the contiguous air-volumes on both sides of the transducer to the response of the system ($\sigma_0 = 72$ mN/m; AM = 250 steps; $R_c = 0.83$ mm; $R_0 = 1.1$ mm).

and the corresponding $\lambda_{\text{critical}}$ (reference syringe amplitude) to compensate the equilibrium surface tension effect is:

$$\lambda_{critical} = \left(\frac{k_3}{V_{R_0}} - \frac{k_1}{V_{X_0}}(N+1) \right) \times \left(\frac{k_2}{V_{X_0}} (N+1) - \frac{k_4}{V_{R_0}} \right)^{-1} \quad (32a)$$

where

$$N = -\left(\frac{k_1 u}{V_{X_0}} - \frac{k_3 u}{V_{R_0}} \right)\left(\frac{2\sigma_0}{R_0^2} + \frac{k_1 u}{V_{X_0}} \right)^{-1}$$

Interestingly, $\lambda_{\text{critical}}$ is found to be independent from the frequency and amplitude of the oscillation and depend only on the physical parameters of the system. Fig. 4 displays the strong dependence of $\lambda_{\text{critical}}$ on the bubble radius and the air volume in the measurement side of the transducer, V_X^a. For these calculations $K_m = 0.19$ μl/Pa, and $V_R^a = 4650$ μl. Extrapolating lines beyond the limits of Fig. 4 reveals that for each R_0 there must exist a value of V_X^a at which the surface tension effect under quasi-static conditions is compensated without moving the reference syringe at all ($\lambda_{\text{critical}} = 0$). The same also holds for each V_R^a, as shown in Fig. 5. Proper selection of the ratio V_R^a/V_X^a for a given value of V_X^a leads to $\Delta P_{\max} = 0$ without using any compensatory pressure signal. Note, that for Karapantsios's experimental configuration where $V_X^a = 1735$ μl and $V_R^a/V_X^a \approx 2.7$ (arrow in figure) such a compensation is needed.

Fig. 6a,b demonstrates how the experimentally measured $\Delta P_{\max}$ and φ are expected to vary with respect to the oscillation frequency, for different values of intrinsic dilatational viscosity. Clearly, the phase lag between the pressure signal and the measurement syringe pulsation, Fig. 6b, is a more sensitive indicator of surface viscosities around 1 mNs/m whereas for viscosity values of about 10 mNs/m both variables are capable of giving reliable estimates. For surfaces with a viscosity of 100 mNs/m, or more, both quantities become gradually insensitive to detect a varying response as the frequency increases. However, for a system of practical interest, the lower viscosity range is expected to represent the interface. In this case,

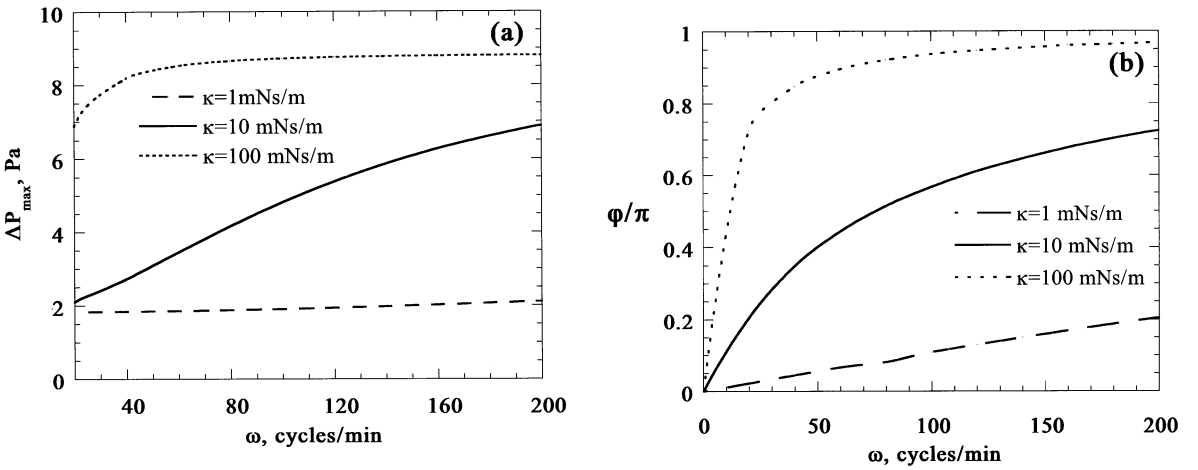

Fig. 6. Effect of surface dilatational viscosity on bubble dynamics: (a) maximum pressure difference during the pulsation, (b) phase lag between pressure signal and movement of the measuring-side syringe ($\sigma_0 = 72$ mN/m; AM = 250 steps; $R_c = 0.83$ mm; $R_0 = 1.2$ mm).

the phase lag between the bubble pressure and the syringe pulsation, φ, can give quite accurate results in predicting intrinsic dilatational viscosity values.

The radius of the capillary tube, to which the bubble is attached, seems to have minor importance to the sensitivity of the technique (graphs not shown due to space limitations). This is particularly true at the low surface dilatational viscosity range. Of course, the use of a smaller radius capillary tube allows us to experiment with smaller size bubbles which are still larger than a hemisphere. Thus, in this indirect way, a smaller capillary tube radius results in higher sensitivity in the surface viscosity measurement.

4. Results and discussion

4.1. Preliminary experiments

From the viewpoint of data interpretation, it is imperative to assess the dynamic behavior of the system during well defined reference experiments before any attempt is made to describe the response of surfactant covered interfaces. Several exploratory blank experiments were performed by Karapantsios [24] with the measurement syringe forced to oscillate at various frequencies while the reference side was kept sealed and where no capillary tube and bubble were attached to the apparatus. The recorded pressure signals appeared very smooth with almost negligible noise. In addition, no phase lag was detected between the syringe movement and the resulting pressure difference whereas pressure variations were accurately represented by Eqs. (8a) and (8b). Similar experiments were also performed with a bubble blown and oscillated in pure water. Again, the signal appeared very smooth and a negligible phase lag was detected. That is, although for the bubble experiments the capillary tube was attached to the apparatus, changing somewhat the geometry of the interior air chamber, no significant pressure noise effect was detected. Therefore, the assumption in the development of the mathematical model of a uniform pressure inside the air chamber of the apparatus appears to be valid for the employed range of oscillation frequencies.

In order to check the validity of the data reduction procedure and of the experimental technique in general, the behavior of pure interfaces must be examined prior to the experiments with surfactant monolayers. A clean surface of a pure Newtonian liquid is not expected to have any rheology in the sense that neither is the surface tension affected by the motion of the surface, nor do the structure and properties of the surface undergo any change,

since in such systems molecular relaxation processes are very fast. However, the experiments conducted by Karapantsios [24] with the pure interfaces, air-water and air-n-hexadecane, showed an unexpected result: although the measured phase lag between the syringe movement and the resulting bubble pressure change was practically zero, as anticipated for a clean interface, the measured bubble pressure change was always lower than expected for a clean interface.

Using the aforementioned measured quantities to solve the present model equations, a zero surface viscosity (due to the observed zero phase lag) but a finite surface elasticity (due to the observed reduced bubble pressure change) are determined. Table 1 displays the measured bubble pressure changes, $\Delta P_\sigma - \Delta P_{max}$, ($\Delta P_\sigma$ is the surface tension contribution) and the corresponding calculated surface elasticity values for Karapantsios's [24] pure air-water and air-n-hexadecane interfaces. The employed frequency of oscillation (cycles/min) and amplitude (steps) of measurement syringe displacement, are also presented. The calculated elasticity values are arbitrarily scattered between ~ 1–11 mN/m. Unfortunately, there are not enough data to infer any reliable frequency or amplitude dependence. These results with pure liquids suggest one of three things: (a) the pure interfaces were not as pure as thought to be, (b) there is a surface dilatational elasticity inherent to the pure interfaces, or (c) there is an additional resistance to bubble expansion in the experiment that is not accounted for in our model, which is of dynamic nature and therefore arises as an apparent dilatational elasticity effect.

Because the water used in the experiments was meticulously and repeatedly redistilled [24], it is difficult to attribute the results to unavoidable contamination. Furthermore, n-hexadecane is a non-polar liquid of relatively low surface tension and therefore is not susceptible to surfactant contamination. Although some investigators [27–30] claim to have measured surface rheological properties for pure liquids, it is difficult to explain from basic principles why such a property should exist in the absence of adsorbed species at the interface. Thus, the third explanation seems to be the most likely at the present time. Although the mathematical model appears to be descriptive of the experiment, the implicit assumption of a non-moving contact line of the oscillating bubble at the capillary tip has not been fully checked. As a matter of fact, particularly acute problems were repeatedly observed by Karapantsios [24] as the bubble approached the hemispherical shape. In summary, his experiments conducted with surfactant-free substrates clearly demonstrate that whereas the measured phase lag between the measuring syringe displacement and the bubble pressure is an accurate indicator of surface viscosity, the bubble pressure signal is highly susceptible to experimental error leading to spurious estimation of surface elasticity.

4.2. Experiments with stearic acid monolayers

Fig. 7a,b and Fig. 8a,b present a selection of bubble pressure and phase lag measurements by Karapantsios [24]. The selection is based primarily on two factors: the bubble pressure measure-

Table 1
System response for pure interfaces

Interface	Oscillation frequency (cycles/min)	Oscillation amplitude (steps of measurement syringe)	$\Delta P_\sigma - \Delta P_{max}$ (Pa)	Interfacial elasticity (mN/m)
Air-water	20	250	0.455	11
Air-water	30	250	0.363	9
Air-water	60	60	0.014	1.3
Air-hexadecane	20	40	0.013	1.2
Air-hexadecane	20	100	0.023	1.1
Air-hexadecane	20	250	0.133	2
Air-hexadecane	30	100	0.025	1.1

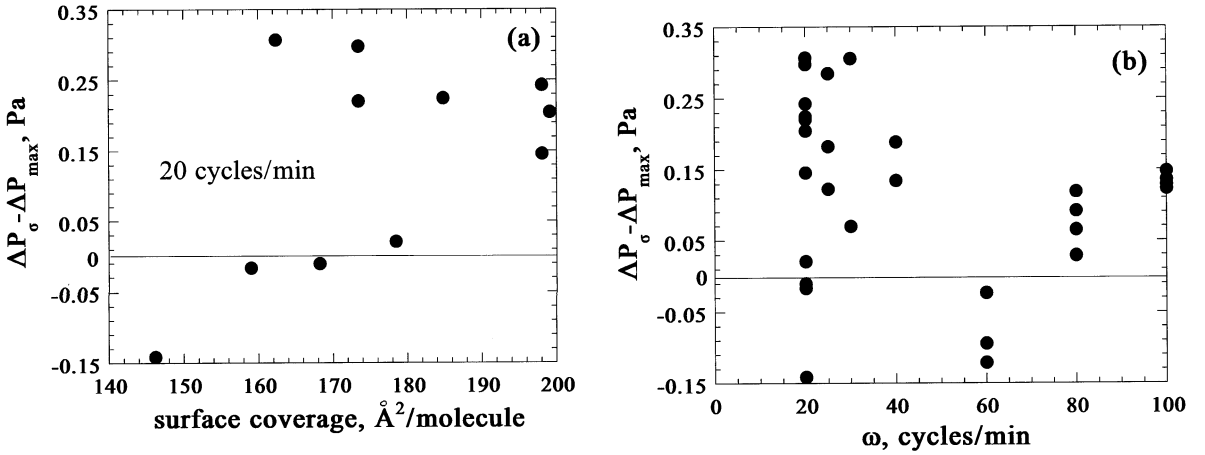

Fig. 7. Bubble pressure change data versus (a) surface coverage and (b) frequency of oscillation.

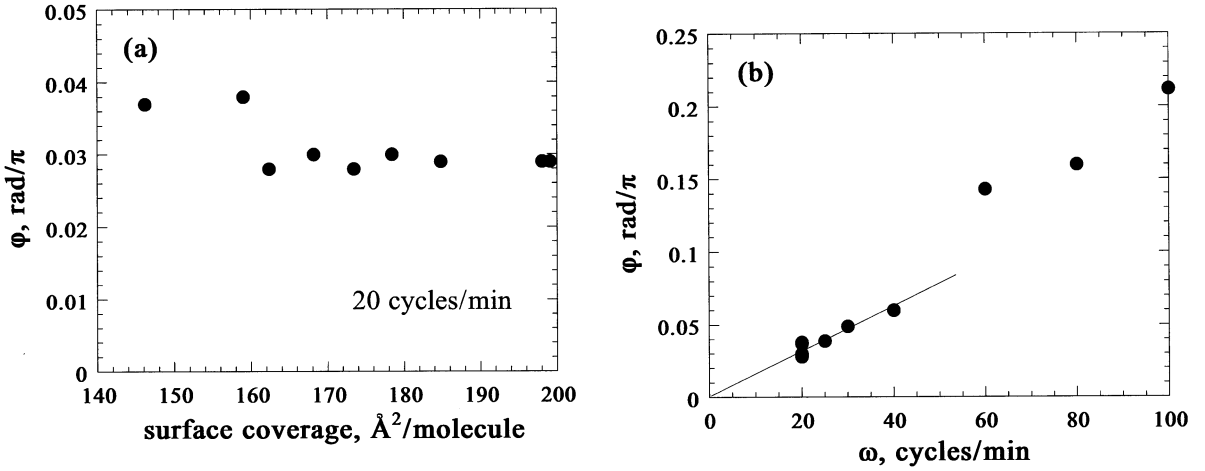

Fig. 8. Phase lag data between pressure signal and measuring-side syringe displacement versus (a) surface coverage and (b) frequency of oscillation.

ments should be accompanied by simultaneous phase lag measurements; data should survive a systematic scrutiny of experimental formal errors with a statistical significance above 95% for the pressure and above 90% for the phase lag. In the phase lag measurements, the relatively large statistical error (worst case at 20 cycles/min) is due to different phase lag values obtained at different locations along the sampled cycles. Apart from that, a more rigorous manipulation of the dynamic behavior of the transducer membrane is employed in reducing the selected data, as explained in Section 3.2.

Fig. 7a,b shows $\Delta P_\sigma - \Delta P_{max}$ data for stearic acid monolayers, versus (a) surface coverage (Å^2/molecule) at 20 cycles/min, and (b) frequency of oscillation for all employed surface coverages (140–200 Å^2/molecule). The values of the pressure data are definitely within the reliable measuring range of the technique. Noticeably, the $\Delta P_\sigma - \Delta P_{max}$ data are arbitrarily scattered without a clear trend in both plots and they attain even negative values which is beyond any physical reasoning (Eq. (22c)). This behavior manifests the achieved degree of accuracy in the sampled pressure data since all negative values should be, at

least, zeros. Goodrich [31] communicated that a scatter of as much as 100% in his data occurred when he was spreading stearic acid from a solvent. He attributed this phenomenon to a possible irreversible interaction between the spreading solvent and the monolayer.

In Fig. 8a the corresponding phase lag ϕ between pressure change $\Delta P_\sigma - \Delta P_{max}$ and syringe displacement V_X^s is drawn as a function of surface coverage at a frequency of 20 cycles/min. The phase lag appears to be almost independent, given the accuracy, of surface coverage when the oscillation frequency is fixed. Fig. 8b demonstrates how this phase lag varies with the frequency of oscillation for all surface coverages. Although there is some scatter, the phase lag appears to monotonically increase with frequency and if the points above 40 cycles/min are excluded, all values lie on a straight line which goes through the origin of the graph, as expected. The points that are excluded may imply that a change in the slope of the previous line occurs for frequencies higher than 40–60 cycles/min.

The data shown in Figs. 7 and 8 are used next, as inputs in the model equations to deduce values of surface elasticity and viscosity. Fig. 9a,b displays the result of these calculations at a frequency of 20 cycles/min. While the surface viscosity values appear to be quite organized and reasonable, in line with Fig. 8, the values of surface elasticity span randomly from 0 to around 6 mN/m, that is, within the range observed for pure interfaces (Table 1). (Note: all negative values of Fig. 7 have been adjusted to zero before solving the model equations.) Combining arguments pertinent to Table 1 and Figs. 7–9, it is realized that the calculated elasticities, dictated chiefly by the measured pressure signal (Section 3), are highly error prone, due perhaps to movement of the bubble centre during the oscillation, and it is rather appropriate at this stage to assume that the present monolayer covered interfaces have approximately zero surface elasticity, akin to pure interfaces.

Fig. 10a,b presents surface viscosity values obtained from the solution of the model equations subject to the assumption that the surface elasticity is zero for all runs. At 20 cycles/min and for the range of the employed surface coverages, the intrinsic dilatational viscosity appears to be virtually constant around the value 1.3 mNs/m. Moreover, the calculated values, despite the small scatter, exhibit a slight but gradually increasing trend as the oscillation frequency increases. This situation is very much like the behavior of a one-element Maxwell surface model at low rates of deformation as also mentioned by Gottier et al. [21]. Calculations of molecular size indicate that the hydrocarbon chains of the adsorbed molecules of stearic acid may overlap about half their chain

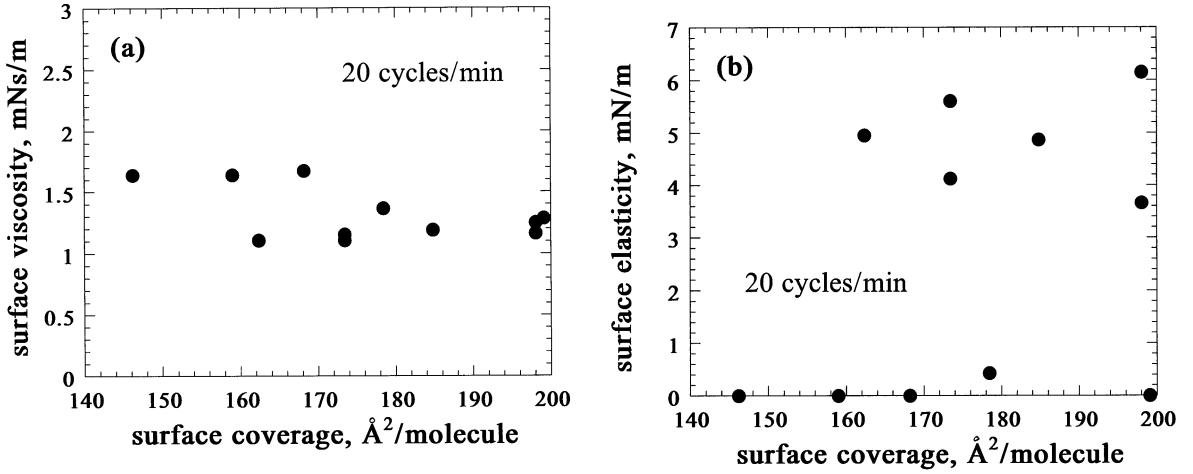

Fig. 9. Calculated dilatational (a) surface viscosity and (b) surface elasticity values versus surface coverage at 20 cycles/min for stearic acid monolayers.

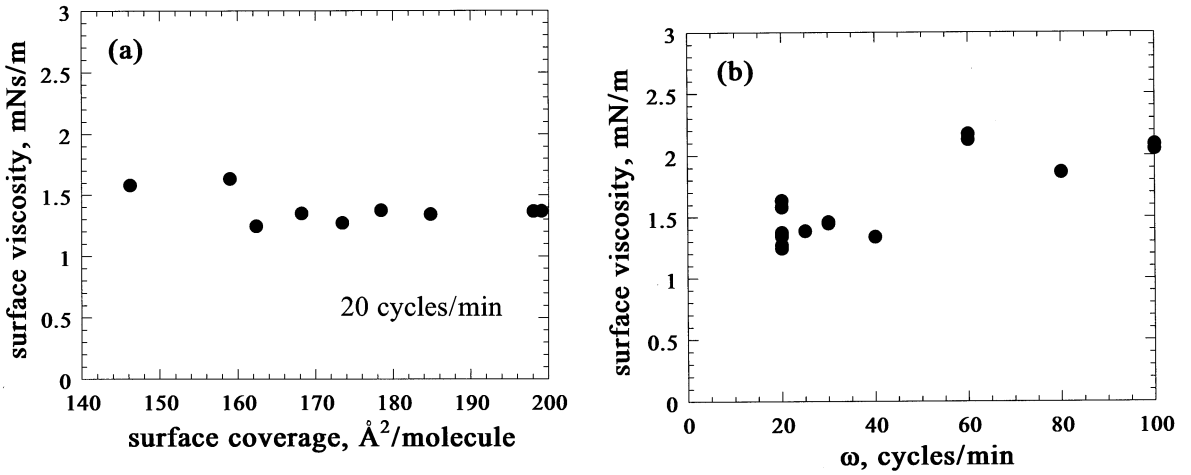

Fig. 10. Calculated dilatational surface viscosity values versus (a) surface coverage and (b) frequency of oscillation when surface elasticity is set equal to zero.

length. This extent of chain-chain interaction may be responsible for the observed frequency dependence of surface viscosity.

Very few studies provide surface rheological data for stearic acid monolayers, so comparison is indeed limited. Mann and Hansen [32] investigating the propagation characteristics of capillary ripples, reported a purely elastic behavior of stearic acid monolayers in experiments conducted in a Langmuir trough. Working at frequencies of 200–1500 cycles per second they measured a compositional dilatational elasticity of about 100 mN/m. Maru and Wasan [2] used the oscillating barrier technique in a Langmuir trough and calculated intrinsic surface dilatational viscosities in the range 0.01 to 0.3 mNs/m, at surface coverages between 35 and 43.8 Å^2 per molecule and oscillation frequencies between 2.5 and 9.7 cycles/min. Although they present very few experimental data points, the indication is that the intrinsic surface dilatational viscosity increases with decreasing surface coverage and decreasing oscillation frequency. Both these observations hold for monolayers much denser than ours so it is rather inappropriate to make direct comparisons. Langevin [33] employing a light-scattering technique reported an intrinsic dilatational viscosity of approximately 0–0.001 mNs/m for surface pressures lower than 1 mN/m. Unfortunately, these data suffer from considerable signal-to-noise ratio and possible distortion which diminish their reliability.

5. Conclusions

To infer interfacial dilatational properties from the response of a modified version of the oscillating bubble technique, a mathematical model is developed incorporating both compositional (Gibbs) elasticities and intrinsic dilatational viscosities. The dilatational rheological properties of surfaces covered with stearic acid monolayers are calculated from two simultaneously measured experimental parameters: the bubble pressure change during the oscillation and the phase lag between bubble pressure and position of the oscillation generating syringe. For the experiments encountered here it is found that phase lag measurements are sufficiently reliable indicators of interfacial rheology in contrast to bubble pressure changes which appear quite susceptible to error. As part of the effort to develop the appropriate mathematical model, various physical properties and experimental parameters that have a significant contribution to the response of the bubble during the oscillation are examined.

New data are calculated from previous measurements by Karapantsios [24], conducted with stearic acid monolayers spread onto bubble sur-

faces with surface coverages between 140 and 200 Å^2/molecule and oscillation frequencies between 20 and 100 cycles/min. For this range of experimental parameters, the calculated intrinsic dilatational surface viscosity lies between 1 and 2 mNs/m without any strong evidence of a dilatational surface elasticity contribution. Furthermore, it is found that for a fixed frequency of oscillation the dilatational surface viscosity is essentially constant throughout the employed surface coverages but gradually increases as the oscillation frequency increases.

In summary, the modified oscillating bubble technique and the accompanying mathematical analysis developed in this work is a very promising method for measuring surface dilatational viscosity. The technique is simple and the analysis avoids all the ambiguities and drawbacks of previous efforts.

References

[1] H.C. Maru, V. Mohan, D.T. Wasan, Chem. Eng. Sci. 34 (1979) 1283.
[2] H.C. Maru, D.T. Wasan, Chem. Eng. Sci. 34 (1979) 1295.
[3] R. Miller, R. Wüstneck, J. Krägel, G. Kretzschmar, Colloids Surfaces A: Physicochem. Eng. Aspects 111 (1996) 75.
[4] A.W. Adamson, Physical Chemistry of Surfaces, Wiley, New York, 1982.
[5] F.H. Adams, G. Enhorning, Acta Physiol. Scand. 68 (1966) 23–27.
[6] H. Slama, W. Schoedel, E. Hansen, Pflug. Arch. 322 (1971) 355.
[7] G. Enhorning, J. Appl. Physiol. 43 (1977) 198.
[8] G. Kretzschmar, K. Lunkenheimer, Ber. Bunsenges. Phys. Chem. 74 (1970) 1064.
[9] K. Lunkenheimer, G. Kretzschmar, Z. Phys. Chem. (Leipzig) 256 (1975) 593.
[10] K.-D. Wantke, R. Miller, K. Lunkenheimer, Abh. Akademie der Wiss. DDR Abt. Mathematik, Naturwiss. Tech., 1N, 439 (1977) 1976.
[11] K.-D. Wantke, R. Miller, K. Lunkenheimer, Z. Phys. Chem. (Leipzig) 261 (1980) 1177.
[12] K. Lunkenheimer, C. Hartenstein, R. Miller, K.D. Wantke, Colloids Surfaces 8 (1984) 271.
[13] C.H. Chang, E.I. Franses, J. Colloid Interface Sci. 164 (1994) 107.
[14] C.H. Chang, E.I. Franses, Chem. Eng. Sci. 49 (1994) 313.
[15] R.L. Kao, D.A. Edwards, D.T. Wasan, E. Chen, J. Colloid Interface Sci. 148 (1992) 247.
[16] R.L. Kao, D.A. Edwards, D.T. Wasan, E. Chen, J. Colloid Interface Sci. 148 (1992) 257.
[17] D.O. Johnson, K.J. Stebe, J. Colloid Interface Sci. 182 (1996) 526.
[18] K.D. Wantke, K. Lunkenheimer, C. Hartenstein, C. Hempt, J. Colloid Interface Sci. 159 (1993) 28.
[19] H. Fruhner, K. Lunkenheimer, R. Miller, Proceedings of the IXth European Symposium on Gravity-Dependent Phenomena in Physical Sciences, Springer-Verlag, Berlin, 1996, pp. 41–50.
[20] H. Fruhner, K.D. Wantke, Colloids Surfaces A: Physicochem. Eng. Aspects 114 (1996) 53.
[21] G.N. Gottier, N.R. Amundson, R.W. Flumerfelt, J. Colloid Interface Sci. 114 (1986) 106.
[22] D.O. Johnson, K.J. Stebe, J. Colloid Interface Sci. 168 (1994) 21.
[23] Y.T. Ko, Ph.D. Thesis in Chemical Engineering, University of Rochester, Rochester, NY, 1986.
[24] T.D. Karapantsios, M.S. Thesis, University of Rochester, Rochester, NY, 1989.
[25] T.D. Karapantsios, H.J. Palmer, 63rd Annual Colloid and Surface Science Symposium of The American Chemical Society, Seattle, WA, 143, June, 1989, 1989, p. 143.
[26] L.E. Scriven, Chem. Eng. Sci. 12 (1960) 98.
[27] J.A. Mann, J.F. Baret, F.J. Dechow, R.S. Hansen, J. Colloid Interface Sci. 37 (1971) 14.
[28] T.E. Ramabhadran, C.H. Byers, J.C. Friedly, AIChE J. 22 (1976) 872.
[29] D. Byrne, J.C. Earnshaw, J. Colloid Interface Sci. 74 (1980) 467.
[30] D. Byrne, J.C. Earnshaw, J. Phys. D: Appl. Phys. 12 (1979) 1145.
[31] F.C. Goodrich, J. Phys. Chem. 66 (1858) 1962.
[32] J.A. Mann, R.S. Hansen, J. Colloid Interface Sci. 18 (1963) 805.
[33] D. Langevin, J. Colloid Interface Sci. 80 (1981) 412.